Published OnlineFirst July 27, 2010; DOI:10.1158/0008-5472.CAN-10-0475

Therapeutics, Targets, and Chemical Biology

Cancer Research

The Human WRN and BLM RecQ Helicases Differentially Regulate Cell Proliferation and Survival after Chemotherapeutic DNA Damage

Frances J. Mao[1], Julia M. Sidorova[1], Julia M. Lauper[1], Mary J. Emond[2], and Raymond J. Monnat[1,3]

Abstract

Loss-of-function mutations in the human RecQ helicase genes *WRN* and *BLM* respectively cause the genetic instability/cancer predisposition syndromes Werner syndrome and Bloom syndrome. To identify common and unique functions of WRN and BLM, we systematically analyzed cell proliferation, cell survival, and genomic damage in isogenic cell lines depleted of WRN, BLM, or both proteins. Cell proliferation and survival were assessed before and after treatment with camptothecin, *cis*-diamminedichloroplatinum(II), hydroxyurea, or 5-fluorouracil. Genomic damage was assessed, before and after replication arrest, by γ-H2AX staining, which was quantified at the single-cell level by flow cytometry. Cell proliferation was affected strongly by the extent of WRN and/or BLM depletion, and more strongly by BLM than by WRN depletion ($P = 0.005$). The proliferation of WRN/BLM-codepleted cells, in contrast, did not differ from BLM-depleted cells ($P = 0.34$). BLM-depleted and WRN/BLM-codepleted cells had comparably impaired survival after DNA damage, whereas WRN-depleted cells displayed a distinct pattern of sensitivity to DNA damage. BLM-depleted and WRN/BLM-codepleted cells had similar, significantly higher γ-H2AX induction levels than did WRN-depleted cells. Our results provide new information on the role of WRN and BLM in determining cell proliferation, cell survival, and genomic damage after chemotherapeutic DNA damage or replication arrest. We also provide new information on functional redundancy between WRN and BLM. These results provide a strong rationale for further developing WRN and BLM as biomarkers of tumor chemotherapeutic responsiveness. *Cancer Res; 70(16); 6548–55.* ©2010 AACR.

Introduction

The human RecQ helicases are members of a deeply conserved protein family that plays important, albeit poorly understood, roles in DNA metabolism, genetic stability, and response to DNA damage (1, 2). Germline loss-of-function mutations in three human RecQ helicase genes, *WRN, BLM*, and *RECQL4*, respectively cause Werner syndrome, Bloom syndrome, and the subset of Rothmund-Thomson syndrome associated with a high risk of osteosarcoma. These genetic instability/cancer predisposition syndromes also have different developmental or acquired features. Werner syndrome patients develop features resembling premature aging beginning in the second decade of life (3). Bloom syndrome patients, in contrast, are proportionately small from birth, display sun sensitivity and hypopigmented and hyperpigmented skin lesions, are often immunodeficient, and have reduced fertility (4). Rothmund-Thomson syndrome patients are typically short with sparse hair and eyebrows; have variable skeletal, dental, and nail abnormalities; and develop a persistent skin rash in infancy together with a high risk of juvenile ocular cataracts (5). Epigenetic loss of expression of RecQ helicases may also be linked to human disease. For example, epigenetic silencing of WRN expression has been documented and is frequent in common adult epithelial malignancies such as colorectal cancer (6, 7). No human disease has been linked thus far to mutation or epigenetic inactivation of the two other human RecQ helicase genes, *RECQL* or *RECQL5* (1, 2).

All five human RecQ proteins share a conserved helicase domain that encodes DNA-dependent ATPase and 3′-to-5′ helicase activities. WRN also encodes a 3′-to-5′ exonuclease activity in an NH_2-terminal domain. Purified human RecQ helicases preferentially bind and unwind, and in the case of WRN also degrade, partially double-stranded DNA molecules including model replication forks, D- and T-loops or synthetic Holliday junctions, and highly structured DNAs such a G-quadruplexes. Several human RecQ helicases also possess DNA strand annealing activity (1, 2, 8). Functional correlates of these activities include a requirement for RecQ helicases in homology-dependent recombination, in replication initiation,

Authors' Affiliations: Departments of [1]Pathology, [2]Biostatistics, and [3]Genome Sciences, University of Washington, Seattle, Washington

Note: Supplementary data for this article are available at Cancer Research Online (http://cancerres.aacrjournals.org/).

Current address for F.J. Mao: Cleveland Clinic Lerner School of Medicine, Cleveland, Ohio.

Corresponding Author: Raymond J. Monnat, Department of Pathology, University of Washington, Box 357705, Seattle, WA 98195-7705. Phone: 206-616-7392; Fax: 206-543-3967; E-mail: monnat@u.washington.edu.

doi: 10.1158/0008-5472.CAN-10-0475

Published OnlineFirst July 27, 2010; DOI:10.1158/0008-5472.CAN-10-0475

in replication restart or fork elongation, and in DNA repair (1, 2, 9–11).

To delineate redundant and unique *in vivo* functions of WRN and BLM, we systematically analyzed cell proliferation, genomic damage as assessed by γ-H2AX staining, and cell survival in isogenic human cell lines depleted of WRN and/or BLM, before and after treatment with DNA-damaging chemotherapeutic drugs. Our results provide new information on the role of WRN and BLM in determining the response to chemotherapeutic damage and on functional redundancy between WRN and BLM.

Materials and Methods

Cells and cell culture

The SV40-transformed GM639 human fibroblast cell line developed from a normal donor was originally obtained from the Coriell Institute Cell Repositories (Camden, NJ) in 1990. GM639-cc1 is a clonal derivative of GM639 that carries an integrated copy of the pNeoA direct repeat homologous recombination reporter plasmid (12). The human osteosarcoma cell line U-2 OS (13) was obtained from the American Type Culture Collection in 2008. GM639 cells are functionally TP53(−), whereas U-2 OS cells express TP53 protein and are functionally TP53(+). Cell lines were initially DNA fingerprinted and screened to verify the absence of *Mycoplasma* infection using PCR kits obtained from the Coriell Institute Cell Repositories. Subsequent fingerprinting and *Mycoplasma* screening verifications have been performed by the University of Missouri Research Animal Diagnostic Laboratory (http://www.radil.missouri.edu/). Recently thawed aliquots of both lines were used for all experiments. GM639-cc1 cells were grown in DMEM and U-2 OS cells in McCoy's 5A medium (MediaTech CellGro) in a humidified 37°C, 7% incubator. Both growth media were supplemented with 4,500 mg/L glucose, 10% (v/v) fetal bovine serum (FBS; Hyclone), and penicillin (100 units/mL) and streptomycin sulfate (100 mg/mL; Invitrogen).

Drugs and dyes

Stock solutions of *cis*-diamminedichloroplatinum(II) (CDDP or *cis*-Pt; 2 mmol/L in 0.9% NaCl), camptothecin (CPT; 1 mmol/L in DMSO), hydroxyurea (HU; 1 mol/L in PBS), 5-fluorouracil (5-FU; 1 mg/mL in DMSO), and 5-bromodeoxyuridine (BrdUrd; 10 mmol/L in sterile water) were stored at −20°C and diluted just before use. Propidium iodide (10 mg/mL in PBS) was stored at 4°C in the dark, and 4,6′-diamidino-2-phenylindole (DAPI; 1 mg/mL) at −20°C. DAPI was obtained from Accurate Chemical and Scientific Corp. All other chemicals and drugs were obtained from Sigma-Aldrich.

Cell proliferation and survival assays

Population-based cell proliferation assays were performed by plating 10^4 cells per well in six-well plates (9.1 cm^2/well). Duplicate wells were trypsinized and counted every 3 days. Cell survival was quantified by colony-forming efficiency (CFE), determined as previously described (12). In brief, 100 to 500 control cells or 4,000 to 20,000 RecQ-depleted cells per well were plated in six-well plates 24 hours before drug treatment, then treated for 24 hours, followed by 8 days of growth in the absence of drug before crystal violet staining to identify colonies containing ≥6 cells.

shRNA-mediated depletion of WRN and BLM

We screened *WRN*- and *BLM*-specific shRNAs designed by The RNAi Consortium (TRC; http://www.broad.mit.edu/rnai/trc/lib) or by Rosetta Inpharmatics, Inc., to identify shRNAs that reproducibly depleted WRN or BLM when expressed from pLKO.1, a lentiviral expression vector containing a human U6 promoter (http://www.broad.mit.edu/genome_bio/trc/protocols/pLKO1.noStuffer.pdf; ref. 14). pLKO.1 shRNA vectors (Fig. 1A) were packaged by cotransfecting pLKO.1 DNA with packaging plasmid pCMV-dR8.2 dvpr and envelope plasmid pCMV-VSVG (kindly provided by Robert Weinberg, Whitehead/MIT, Cambridge, MA) into human 293T cells as previously described (15). Viral supernatants were filtered through a 45-μm filter and stored at −80°C until use. shRNA-mediated depletions were performed by transducing cells with shRNA lentivirus for 48 hours, followed by an additional 96 hours of puromycin selection (1.5–2.0 μg/mL). Depletions were quantified by Western blot analysis (Fig. 1B). Controls included cells transduced with pLKO.1 vector DNA alone or with pLKO.1 expressing a scrambled shRNA with no known target sequence in the human genome (plasmid 1864, "scramble shRNA"; Addgene). Codepletions were achieved by simultaneously transducing cells with *WRN*- and *BLM*-specific shRNA lentiviruses.

Western blot analyses

Solubilized cell pellets (~1 × 10^6 cells), prepared as previously described (16, 17), were resolved by SDS-PAGE (Invitrogen, Nu-PAGE) before transfer onto a polyvinylidene difluoride membrane (Bio-Rad). WRN protein was detected with mouse monoclonal anti-WRN primary antibody 195C

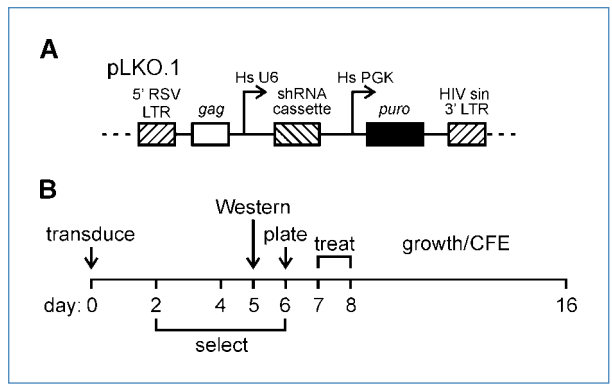

Figure 1. RNA interference–mediated depletion of WRN and BLM. A, pLKO.1 lentiviral vector used for shRNA expression. LTR, 5′ RSV and 3′ self-inactivating HIV long terminal repeats; Hs U6, human U6 promoter; Hs PGK, human phosphoglycerate kinase promoter; puro, puromycin resistance gene. B, experimental protocol for the generation or use of WRN- and/or BLM-depleted cells. Depletion of WRN and BLM was maximal from 5 to 6 d after transduction and persisted for >14 d (refs. 15, 16; additional results not shown).

Published OnlineFirst July 27, 2010; DOI:10.1158/0008-5472.CAN-10-0475

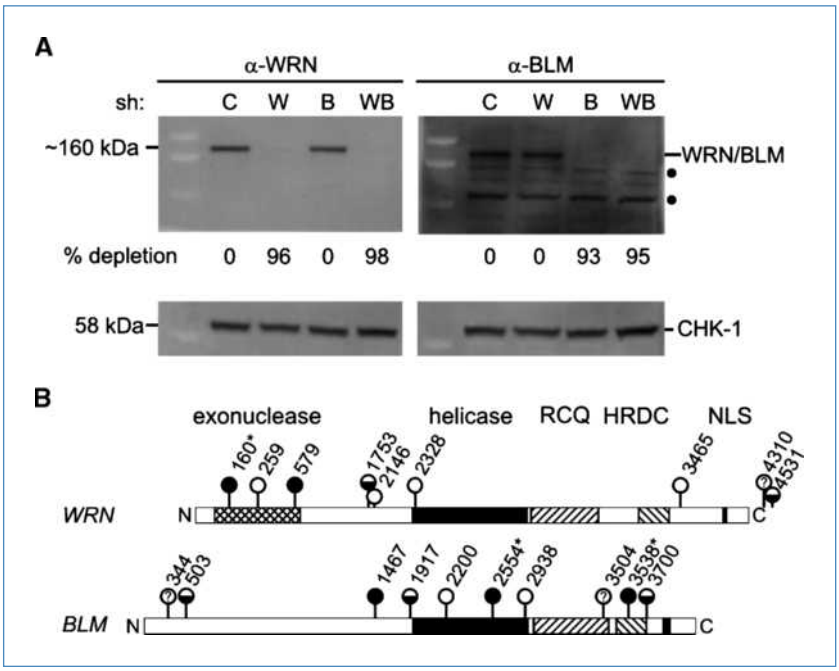

Figure 2. Lentiviral shRNAs selectively deplete or codeplete WRN and BLM. A, Western blot analysis of GM639 cells after *WRN*- and/or *BLM*-specific shRNA expression. C, pLKO.1 vector control; W, shWRN579; B, shBLM2554; W + B, shWRN579 and shBLM2554, where individual shRNAs are numbered from their 5′ end in the corresponding *WRN* or *BLM* cDNA sequence (see part B). The predicted molecular weight of *WRN* is 162 kDa and *BLM* is 159 kDa. ●, nonspecific cross-reacting bands detected by our polyclonal *BLM* antisera. CHK1 protein was used as a loading control. B, summary of shRNAs screened for ability to deplete *WRN* or *BLM* proteins, where symbols indicate extent of depletion: ●, >90% depletion; ◒, 20–90% (partial) depletion; ○, <20% or no detectable depletion; ⓘ, inconclusive data. *, shRNAs verified in both retroviral and lentiviral vectors.

(kindly provided by Dr. Patricia Opresko, University of Pittsburgh, Pittsburgh, PA; ref. 18). BLM protein was detected using affinity-purified rabbit polyclonal anti-BLM antisera directed against the BLM COOH-terminal peptide KPINRPFLKPSYAFS (additional results not shown). Human CHK1 protein was detected with an anti-Chk1 mouse monoclonal primary antibody (Santa Cruz). Bound antibodies were detected by enhanced chemiluminescence (GE Healthcare; Fig. 2A). Blots were scanned and quantified using a Storm Phosphorimager and ImageQuant software (Molecular Dynamics) as previously described (16).

Flow cytometric analysis of γ-H2AX–stained cells

Genomic damage was quantified by flow cytometric analysis of cellular γ-H2AX staining as previously described (19). In brief, 1×10^5 to 2×10^5 cells per well were plated in six-well plates before treatment with HU for 2 to 8 hours. Cells were scrape-harvested, washed twice in 1× PBS, fixed with 1-mL cold 66% ethanol/PBS, and stored at 4°C until analyzed. Fixed cells were resuspended in TBS [25 mmol/L Tris-HCl (pH 7.4), 137 mmol/L NaCl, 5 mmol/L KCl] supplemented with 4% FBS and 0.1% Triton X-100, incubated on ice for 10 minutes, and stained for 1 hour with a mouse monoclonal anti–phospho-histone H2AX (Ser139) primary antibody (clone JBW301, Millipore) for 1 hour. Bound antibody was detected by staining for 1 hour with a goat anti-mouse Alexa 488–conjugated-secondary antibody (Molecular Probes, A1100110C). Cells resuspended in TBS were stained with DAPI (10 μg/mL) before flow cytometric analysis on an Influx flow cytometer (Cytopeia, Inc.). Control cells (pLKO.1 vector only or pLKO.1 scrambled shRNA) were used to define baseline staining set to include 1% of the cell population in the positive cell fraction (gate 1). A second gate included all cells while excluding cell debris (gate 2). The same gating was used for all samples within an experiment. Gate 1 versus gate 2 ratios defined the "percent γ-H2AX–positive" cells, and "fold inductions" were calculated by dividing experimental by control, γ-H2AX–positive cell frequencies.

Cell cycle distribution determined by BrdUrd labeling and flow cytometry

RecQ-depleted and control cells were labeled with 50 mmol/L BrdUrd for 2 hours, then harvested as previously described (15). BrdUrd content was determined by fixing cells in cold 66% ethanol/PBS, denaturing in 2 N HCl/0.5% Triton X-100 for 30 minutes each, and then neutralizing samples with 100 mmol/L Na borate (pH 8.5). Immunostaining to detect incorporated BrdUrd was done for 1 hour each at 4°C in the dark with mouse anti-BrdUrd primary antibody (347580, BD Biosciences), followed by Alexa 488–conjugated antimouse secondary antibody (Molecular Probes A1100110C). Cells were strained with propidium iodide (10 μg/mL) in PBS containing 100 μg/mL RNase A before analysis on an Influx flow cytometer. Data analyses were done using Summit software (Dako). Cell cycle fractions were estimated using FCS Express (De Novo Software) or M-cycle (Phoenix Flow Systems).

Statistical analysis of cell proliferation, survival, and γ-H2AX straining

Regression modeling was used as the most rigorous way to analyze outcomes as a function of RecQ depletion type while controlling for time, within-experiment correlations, extent of depletion, drug, and drug dose. This approach allowed us to analyze primary proliferation, survival, or staining data to identify significant differences while correcting for interactions between variables and for multiple testing. Differences were considered significant if they met a P value that was Bonferroni corrected for multiple testing by experiment type

Published OnlineFirst July 27, 2010; DOI:10.1158/0008-5472.CAN-10-0475

to preserve a family-wise type I error rate of 0.05. These corrected *P* values were as follows: cell proliferation, $P = 0.012$; cell survival, $P = 0.00096$; and γ-H2AX induction, $P = 0.007$. Analyses of log cell counts and γ-H2AX straining were fitted as a linear function of time. Data for survival of drug-treated U-2 OS cells with fewer than 500 cells plated were excluded from regression analysis to avoid generating artificially high colinearity within the treated survival design matrix. CFE outcomes were normalized to zero-dose CFE by including the latter in the regression model. This approach requires fewer modeling assumptions than using a "ratio of ratios" approach (20) and thus avoids the high variability generated when dividing by small numbers. Differences between depletion states (control, scrambled shRNA, WRN or BLM depleted, and WRN/BLM codepleted) were tested after adjusting for dose and experiment.

Results

Depletion of WRN and BLM from human fibroblasts

We identified two *WRN*-specific and three *BLM*-specific shRNAs that reproducibly depleted their respective target proteins in different cell types by ≥90%. We also identified two additional *WRN*-specific and three additional *BLM*-specific shRNAs that partially depleted WRN or BLM by 30% to 70% (Figs. 1 and 2; additional results not shown). Western blot analyses indicated that both WRN and BLM were maximally depleted by day 6 after transduction and remained depleted at ≥90% for at least 25 days (Fig. 2A; Supplementary Fig. S1; refs. 13–15; additional data not shown). Cotransduction using the same protocol and shRNA lentiviral stocks led to simultaneous depletion of both WRN and BLM by ≥90% (Fig. 2A).

Cell proliferation as a function of WRN/BLM protein content

Depletion of WRN or BLM from GM639 and U-2 OS cells suppressed cell proliferation in both population-based and clonal proliferation assays. Higher percent depletions were associated with stronger suppression for both WRN and BLM. Cell proliferation was more strongly suppressed by BLM than by WRN depletion as a function of percent depletion over the observed depletion range, and comparable slopes were observed for regression lines that related percent protein depletion to percent proliferative suppression in both population-based and colony-forming assays (Fig. 3). Of note, the proliferation of WRN/BLM-codepleted cells did not differ from that of cells depleted of BLM alone ($P = 0.34$; Fig. 3; Supplementary Fig. S2).

Genomic damage after WRN/BLM depletion

As a measure of genomic damage, we quantified both basal and replication arrest–induced γ-H2AX levels in WRN- and/or BLM-depleted cells. γ-H2AX is a minor histone H2 variant that is phosphorylated on Ser139 in response to replication stress and other types of genomic damage including DNA breakage (21, 22). The primary data presented in Fig. 4 are means and SDs for fold γ-H2AX induction from five independent experiments. All of these data and time points were used to build a regression model to determine the rate of change and whether there were differences in mean fold γ-H2AX induction as a function of time and depletion type. These analyses revealed significantly higher γ-H2AX inductions in all depleted cell types (WRN-depleted, BLM-depleted, or WRN/BLM-codepleted) as compared with controls and no significant difference in γ-H2AX induction between cells depleted of BLM alone and WRN/BLM-codepleted cells

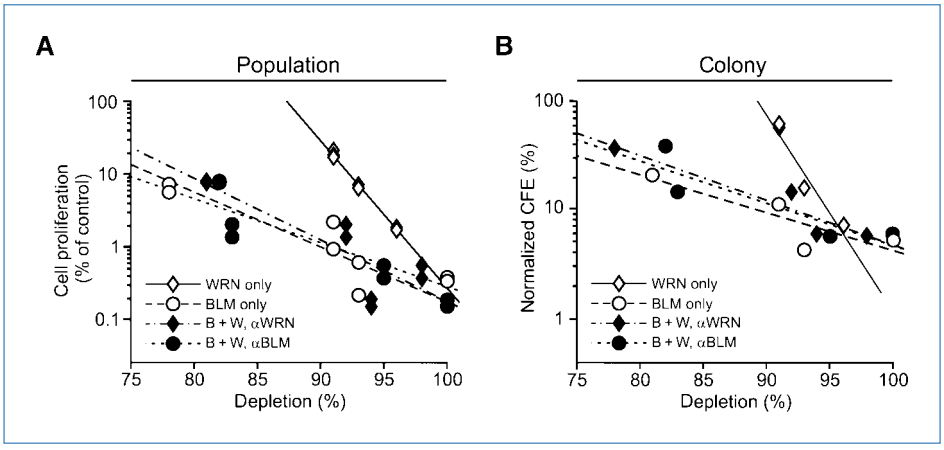

Figure 3. WRN and BLM depletion suppress cell proliferation. A, proliferation of GM639 human fibroblasts depleted of WRN and/or BLM. Open symbols, proliferation measured at day 9 (see Fig. 1B); filled symbols, proliferation at the same time point in codepleted cells where WRN (♦) or BLM (●) depletion was determined by Western blot in four independent experiments. The proliferation of BLM-depleted versus WRN-depleted cells was significantly different ($P = 0.0002$), in contrast to BLM-depleted versus WRN/BLM-codepleted cells ($P = 0.34$). The slopes of regression lines for proliferative suppression as a function of percent depletion were –0.20 and –0.061 $\log_{10}$ units of percent of control per 1% protein depleted for WRN and BLM, respectively. B, colony formation by WRN- or BLM-depleted cells was significantly suppressed as a function of percent depletion ($P = 3.9 \times 10^{-7}$ for WRN and $P = 0.0016$ for BLM), with significantly stronger suppression in BLM- versus WRN-depleted cells ($P = 1.1 \times 10^{-8}$). There was no difference between BLM-depleted and WRN/BLM-codepleted cells in colony-forming ability ($P = 0.45$). Slopes of the regression lines for suppression of CFE as a function of WRN or BLM depletion were –0.18 and –0.035 $\log_{10}$ units of percent of control per 1% of protein depleted, respectively.

Published OnlineFirst July 27, 2010; DOI:10.1158/0008-5472.CAN-10-0475

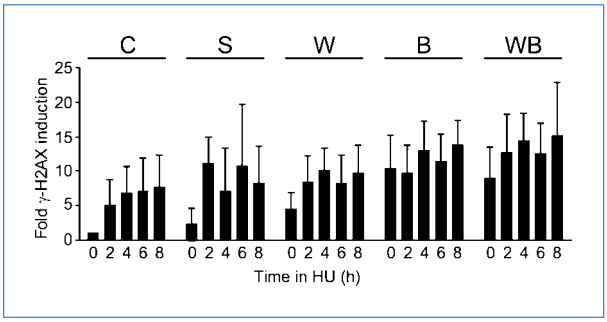

Figure 4. Elevated genomic damage with γ-H2AX staining in HU-arrested WRN- and/or BLM-depleted cells. The bar graphs are primary data from γ-H2AX induction experiments using WRN- and/or BLM-depleted GM639 fibroblasts and replication arrest with 2 mmol/L HU where controls were pLKO.1 vector-only (C) or scrambled shRNA–expressing cells (S). Regression modeling of these data revealed significantly higher staining in WRN- and/or BLM-depleted cells versus either type of control (C or S; $P < 0.01$; Supplementary Table S1) and a linear rate of change in fold γ-H2AX induction as a function of time. BLM-depleted and WRN/BLM-codepleted cells had significantly higher fold inductions in staining than did WRN-depleted cells ($P = 0.0016$ and $P = 2.8 \times 10^{-6}$, respectively) but did not differ from one another ($P = 0.18$; Supplementary Table S1). There was no difference in slopes/rate of change in the induction of H2AX staining over time as a function of depletion type (W, B, or WB). Bars, SD for five independent experiments except for shScr where duplicate values from a single experiment are shown. C, pLKO.1 control vector; S, scrambled shRNA control; W, shWRN579; B, shBLM2554; WB, codepletion with shWRN579 + shBLM2554.

(Supplementary Table S1). The rate of increase in γ-H2AX staining as a function of time in HU was linear and did not differ as a function of depleted protein(s). Differences in γ-H2AX staining among depleted cells were not explained by differences in cell cycle phase distribution, as assessed by BrdUrd labeling (ref. 16; additional results not shown). These results indicate that the depletion of WRN or BLM may lead to genomic damage that can be detected by higher levels of γ-H2AX staining. Comparable results were observed in U-2 OS cells, although these were not formally analyzed as we had fewer data than for GM639 cells (additional results not shown).

Cell survival after WRN/BLM depletion and DNA damage

We quantified cell survival of depleted, isogenic cell lines after treatment with four different cancer chemotherapeutic agents: the topoisomerase I inhibitor CPT, the DNA cross-linking drug *cis*-Pt, the ribonucleotide reductase inhibitor HU, and the antimetabolite and thymidylate synthase inhibitor 5-FU. Primary data from these analyses, performed as CFE assays using GM639 or U-2 OS cells, are shown in Fig. 5. These data were again analyzed by regression modeling to use experimental data across different doses and to correct for potential experimental confounders and for multiple testing.

Depletion of WRN or BLM significantly sensitized GM639 and U-2 OS cells to dose-dependent killing by CPT, cis-Pt, and 5-FU, and BLM-depleted cells to HU (Fig. 5; $P = 0.31$; Table 1; see also ref. 16). Several significant differences in survival were noted between depletion type (WRN or BLM) and by cell line. BLM-depleted GM639 cells had significantly lower survival after CPT or HU treatment than did WRN-depleted cells. In contrast, WRN-depleted U-2 OS cells had significantly lower survival after *cis*-Pt treatment than did BLM-depleted or codepleted cells. Of note, codepletion of

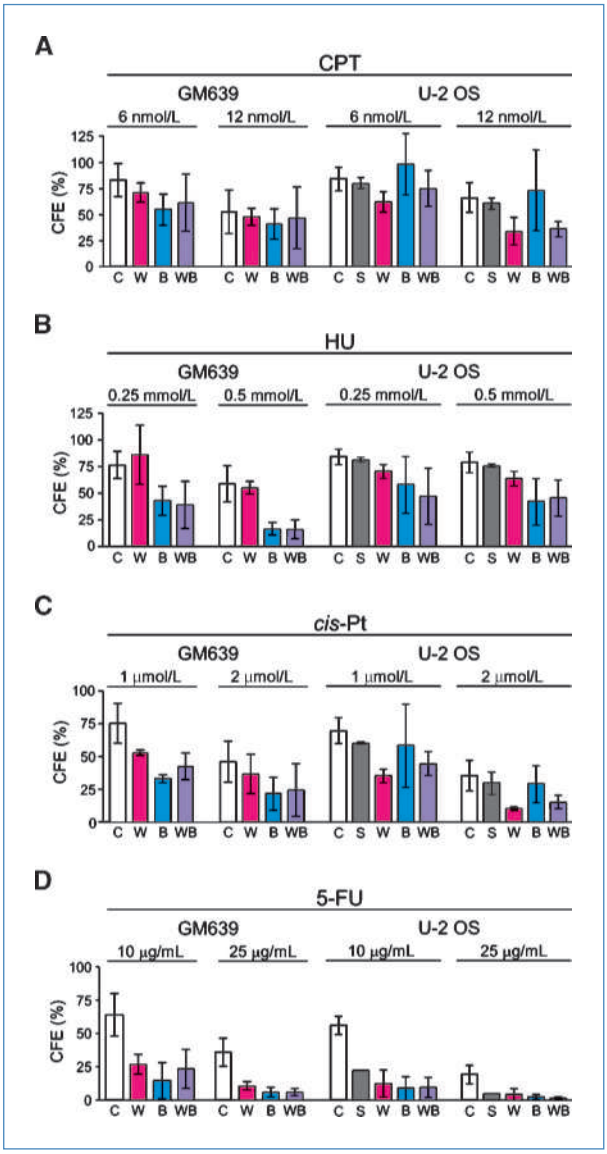

Figure 5. Chemotherapeutic drugs selectively kill WRN- and/or BLM-depleted cells. Columns, mean CFE of depleted and control GM639 and U-2 OS cell lines after 24-h treatment with CPT, HU, *cis*-Pt, or 5-FU from two to five independent experiments; bars, SD. Data were analyzed by regression modeling (Table 1) to account for cell type, depletion type (W, B, or WB), agent, dose, and between-experiment variation. WRN- or BLM-depleted drug-treated cells had significantly lower survival than controls after treatment with CPT, cis-Pt, and 5-FU ($P < 1 \times 10^{-4}$ for all control versus treatment comparisons). WRN-depleted GM639 cells had significantly higher CFE than did BLM-depleted cells after CPT or HU treatment. BLM-depleted and WRN/BLM-codepleted cells had statistically indistinguishable survival with the exception of BLM-depleted U-2 OS versus WB-codepleted cells treated with CPT (Table 1). C, pLKO.1 control vector; S, scrambled shRNA control vector; W, shWRN579; B, shBLM2554; WB, shWRN579 + shBLM2554.

Published OnlineFirst July 27, 2010; DOI:10.1158/0008-5472.CAN-10-0475

Table 1. Regression modeling identifies significant differences in cell survival of WRN- and/or BLM-depleted cells after DNA damage

Agent	Comparison samples*		Cell line	
			GM639	U-2 OS
	S1	S2	*P*†	*P*
CPT	C	W	$<1.0 \times 10^{-16}$‡	2.7×10^{-6}‡
	C	B	$<1.0 \times 10^{-16}$‡	2.2×10^{-6}‡
	C	WB	$<1.0 \times 10^{-16}$‡	4.9×10^{-7}‡
	W	B	6.0×10^{-6}‡	0.064
	W	WB	0.0025	0.55
	B	WB	0.81	9.5×10^{-5}‡
HU	C	W	0.0012§	0.31
	C	B	3.0×10^{-9}‡	5.7×10^{-10}‡
	C	WB	7.0×10^{-11}‡	4.0×10^{-16}‡
	W	B	5.0×10^{-4}‡	0.14
	W	WB	4.0×10^{-5}‡	0.10
	B	WB	0.04	0.37
cis-Pt	C	W	$<1.0 \times 10^{-16}$‡	$<1.0 \times 10^{-16}$‡
	C	B	$<1.0 \times 10^{-16}$‡	$<1.0 \times 10^{-16}$‡
	C	WB	$<1.0 \times 10^{-16}$‡	$<1.0 \times 10^{-16}$‡
	W	B	0.0025	$<1.0 \times 10^{-16}$‡
	W	WB	0.0006‡	$<1.0 \times 10^{-16}$‡
	B	WB	0.22	$<1.0 \times 10^{-16}$‡
5-FU	C	W	$<1.0 \times 10^{-16}$‡	$<1.0 \times 10^{-16}$‡
	C	B	$<1.0 \times 10^{-16}$‡	$<1.0 \times 10^{-16}$‡
	C	WB	$<1.0 \times 10^{-16}$‡	$<1.0 \times 10^{-16}$‡
	W	B	0.013	0.52
	W	WB	0.21	0.13
	B	WB	0.11	0.03

NOTE: CFE data in Fig. 5 were used for the statistical analysis of colony-forming efficiency, which used regression modeling to account for cell type, depletion type (W, B, or WB), agent, dose, and between-experiment variation. Control and depleted cells were treated for 24 h with CPT, HU, *cis*-Pt, or 5-FU.

Abbreviations: S1, sample 1; S2, sample 2; C, pLKO.1 vector–transduced; W, WRN-depleted; B, BLM-depleted; WB, WRN/BLM-codepleted.

*Sample pairs were tested for significance.

†*P* values <0.00096 are significant after Bonferroni correction for multiple testing.

‡Statistically significant difference.

§This *P* value was calculated from 0.5 mmol/L HU data only to avoid introducing artefact.

WRN and BLM did not additively or synergistically sensitize depleted cells to killing by any of the four drugs tested (Fig. 5; Table 1). $P = 0.00096$ was the cutoff for significance in these analyses, corrected for multiple testing to retain a type I error rate of 0.05 (Table 1).

Discussion

To determine how WRN and BLM influence the response to chemotherapeutic drugs, we quantified cell proliferation, genomic damage as assessed by γ-H2AX induction, and cell survival after treating WRN- and/or BLM-depleted cells with four different DNA-damaging chemotherapeutic drugs. Isogenic, WRN- or BLM-depleted or WRN/BLM-codepleted TP53(+) and TP53(−) cell lines were used together with regression modeling to control for important variables including cell line, depleted protein and percent depletion, drug, and drug dose. Codepletion analyses also allowed us to analyze for the first time the functional redundancy of WRN and BLM in isogenic human cell line pairs.

WRN or BLM depletion alone suppressed cell proliferation in both TP53(+) and TP53(−) cell lines (Fig. 3) and increased genomic damage as assessed by γ-H2AX induction both before and after HU-mediated replication arrest (Fig. 4). WRN- or BLM-depleted cells were sensitized to dose-dependent killing by CPT, cis-PT, and 5-FU (see Fig. 5 data and Table 1 statistical analysis). WRN-depleted GM639 cells had significantly higher survival after CPT or HU treatment than did isogenic BLM-depleted cells. Of note, depletion of BLM from WRN-depleted cells sensitized them to HU-mediated cell killing. Conversely, BLM-depleted U-2 OS cells were refractory to CPT killing, but could be sensitized to CPT-mediated cell killing by the depletion of WRN (Fig. 5 data and Table 1 statistical analysis).

These results substantially extend and clarify our understanding of the proliferation and drug sensitivity phenotypes of WRN- or BLM-deficient human cells. Previous work by us and others had documented reduced proliferative potential and DNA damage sensitivity of WRN-deficient, patient-derived fibroblasts, peripheral blood lymphocytes, or B-lymphoblastoid cell lines to *cis*-Pt and CPT. Other reports had documented the selective killing of WRN-deficient cells by 4-nitroquinoline 1-oxide (4-NQO), mitomycin C, and 8-methoxy-psoralen + UV light using chromosomal breakage, colony formation, or flow cytometric assays (12, 16, 23–30). There are inconsistent reports on the HU sensitivity of WRN-deficient cells, together with one or more reports of no selective sensitivity of WRN-deficient, often patient-derived, cells after UV damage or Adriamycin, daunomycin, etoposide, *trans*-Pt, beneril, or mitoxantron treatment (27, 31). Fewer reports have documented the drug sensitivity of BLM-deficient cells. BLM-deficient human lymphoblast and fibroblast cell lines were reported to be selectively killed by UV light or HU (32) and, less consistently, by CPT (25, 33, 34). *Blm*-mutant mouse ES cells seem to be hypersensitive to the intercalating agent ICRF-193 but, in contrast to BLM-deficient human cells, are mildly resistant to CPT and strongly resistant to HU (35).

One unexpected new finding with both mechanistic and clinical implications in our analyses was the marked 5-FU sensitivity of both WRN- and BLM-deficient TP53(+) and TP53(−) cells. There were few prior suggestions that this widely used chemotherapeutic antimetabolite might selectively kill RecQ helicase–deficient human cells. Although the mode of

Published OnlineFirst July 27, 2010; DOI:10.1158/0008-5472.CAN-10-0475

action of FU is still poorly understood (36, 37), loss of WRN or BLM could promote 5-FU cell killing by interfering with DNA replication or by inducing error-prone, homology-dependent recombination. Both DNA replication and recombination have different requirements for RecQ helicase function as discussed above. It should be possible to provide additional mechanistic insight into the 5-FU–mediated killing of WRN- or BLM-deficient cells. DNA replication could be analyzed at the single molecule level with the methods we developed and used to show replication defects in WRN-deficient human cells (15). Similar approaches have also been used to show replication defects in BLM-deficient human cells (9, 38). Recombination defects in 5-FU–treated WRN- or BLM-deficient cells could be quantified and analyzed at the molecular level using recombination reporter substrates of the type originally used to identify the recombination resolution defect in WRN-deficient cells (see, e.g., ref. 12).

Our results provide a first analysis of functional redundancy between WRN and BLM in human cells. Prior analyses of functional redundancy had used Wrn/Blm double-mutant mice or avian DT-40 cells. In contrast, no patient has been identified who lacks more than one of the human RecQ helicases. Wrn/Blm-mutant mice develop strong cellular and organismal phenotypes that resemble Werner syndrome, but only after ≥3 generations in a telomerase-deficient background (39, 40). These experiments thus support the idea that WRN and BLM may act on short or disrupted telomeres to suppress DNA damage responses, genetic instability, and cellular senescence (41, 42). Wrn/Blm-mutant avian DT-40 cells display a proliferation defect and are hypersensitive to CPT (43). Wrn-deficient DT-40 cells, in contrast, are only mildly sensitive to CPT, *cis*-Pt, 4-NQO, and MMS (44, 45), whereas Blm-deficient DT-40 cells have a proliferative defect and are selectively sensitive to etoposide, bleomycin, 4-NQO, UVC irradition, X-irradiation, and HU (46, 47).

We found that codepletion of WRN and BLM in human cells suppressed cell proliferation, led to higher γ-H2AX staining both before and after HU arrest (Figs. 3 and 4), and led to dose-dependent killing of both TP53(+) or TP53 (−) cells by all four chemotherapeutic agents we tested (Fig. 5). An important new finding in these analyses was the lack of additive or synergistic defects in WRN/BLM-codepleted cells. This finding indicates that WRN and BLM may act in a common pathway to suppress genomic damage and ensure cell survival after chemotherapeutic DNA damage. The stronger organismal and cellular phenotype observed after loss of BLM further suggests that BLM may have a disproportionate role in this common functional pathway or may have additional functions that were not readily revealed in our assays (3, 4). One prediction from this model is that somatic cells, stem cells, and tissues from Bloom syndrome patients will display higher levels of cell turnover, mutagenesis, and telomere erosion than comparable cells or tissues from Werner syndrome patients (48).

Our results provide a strong rationale for developing the human RecQ helicases as novel cancer therapeutic biomarkers and targets. RecQ helicase mutations are uncommon in human tumors, but epigenetic loss of expression seems to be frequent in common adult epithelial malignancies such as colorectal cancer (6, 7). Thus, RecQ expression profiling could identify tumors that could be selectively killed by widely used chemotherapeutic agents such as 5-FU, *cis*-Pt, or CPT that selectively kill RecQ-deficient cells. Of note, as shown above, these drugs selectively kill WRN- and/or BLM-deficient cells regardless of TP53 status. Targeting human RecQ helicases may provide a second way to improve cancer chemotherapy. Direct inhibition of WRN or BLM should confer a drug sensitivity profile similar to that observed in RecQ-deficient, transformed human cells. However, this strategy in its simplest form would not confer tumor-specific cell killing *in vivo*. An alternative approach would be to identify drugs or small molecules that inhibit survival pathways required for cell viability in the absence of WRN or BLM (49, 50). Agents that selectively killed RecQ-deficient tumor cells might be useful as monotherapies or in conjunction with lower doses of conventional chemotherapy. Our results and these additional approaches thus might allow highly effective therapies to be designed for cancer patients with RecQ helicase–deficient tumors.

Disclosure of Potential Conflicts of Interest

No potential conflicts of interest were disclosed.

Acknowledgments

We thank the Rabinovitch Lab (Department of Pathology, University of Washington, Seattle, WA) for help with flow cytometric analyses, Alden F.M. Hackmann for data assembly and graphics support, and Carla Grandori and Kiran Dhillon for help in establishing shRNA technology.

Grant Support

National Cancer Institute PO1 award CA77852 (R.J. Monnat) and a Mary Gates Undergraduate Research Fund award (F.J. Mao).

The costs of publication of this article were defrayed in part by the payment of page charges. This article must therefore be hereby marked *advertisement* in accordance with 18 U.S.C. Section 1734 solely to indicate this fact.

Received 02/09/2010; revised 05/24/2010; accepted 06/03/2010; published OnlineFirst 07/27/2010.

References

1. Bohr VA. Rising from the RecQ-age: the role of human RecQ helicases in genome maintenance. Trends Biochem Sci 2008;33:609–20.
2. Chu WK, Hickson ID. RecQ helicases: multifunctional genome caretakers. Nat Rev Cancer 2009;9:644–54.
3. Epstein CJ, Martin GM, Schultz AL, Motulsky AG. Werner's syndrome: a review of its symptomatology, natural history, pathologic features, genetics and relationship to the natural aging process. Medicine 1966;45:177–221.
4. German J. Bloom syndrome: a Mendelian prototype of somatic mutational disease. Medicine 1993;72:393–406.
5. Wang LL, Levy ML, Lewis RA, et al. Clinical manifestations in a cohort of 41 Rothmund-Thomson syndrome patients. Am J Hum Genet 2001;102:11–7.

Published OnlineFirst July 27, 2010; DOI:10.1158/0008-5472.CAN-10-0475

6. Agrelo R, Cheng WH, Setien F, et al. Epigenetic inactivation of the premature aging Werner syndrome gene in human cancer. Proc Natl Acad Sci 2006;103:8822–7.
7. Kawasaki T, Ohnishi M, Suemoto Y, et al. WRN promoter methylation possibly connects mucinous differentiation, microsatellite instability and CpG island methylator phenotype in colorectal cancer. Mod Pathol 2007;21:150–8.
8. Bachrati CZ, Hickson ID. RecQ helicases: suppressors of tumorigenesis and premature aging. Biochem J 2003;374:577–606.
9. Rao VA, Conti C, Guirouilh-Barbat J, et al. Endogenous γ-H2AX-ATM-Chk2 checkpoint activation in Bloom's syndrome helicase-deficient cells is related to DNA replication arrested forks. Mol Cancer Res 2007;5:713–24.
10. Xu X, Rochette PJ, Feyissa EA, Su TV, Liu Y. MCM10 mediates RECQ4 association with MCM2-7 helicase complex during DNA replication. EMBO J 2009;28:3005–14.
11. Thangavel S, Mendoza-Maldonado R, Tissino E, et al. The human RECQ1 and RECQ4 helicases play distinct roles in DNA replication initiation. Mol Cell Biol 2009;30:1382–96.
12. Saintigny Y, Makienko K, Swanson C, Emond MJ, Monnat RJ, Jr. Homologous recombination resolution defect in Werner syndrome. Mol Cell Biol 2002;22:6971–8.
13. Pontén J, Saksela E. Two established *in vitro* cell lines from human mesenchymal tumours. Int J Cancer 1967;2:434–47.
14. Moffat J, Grueneberg DA, Yang X, et al. A lentiviral RNAi library for human and mouse genes applied to an arrayed viral high-content screen. Cell 2006;124:1283–98.
15. Sidorova JM, Li N, Folch A, Monnat RJ, Jr. The RecQ helicase WRN is required for normal replication fork progression after DNA damage or replication fork arrest. Cell Cycle 2008;7:796–807.
16. Dhillon KK, Sidorova J, Saintigny Y, et al. Functional role of the Werner syndrome RecQ helicase in human fibroblasts. Aging Cell 2007;6:53–61.
17. Swanson C, Saintigny Y, Emond MJ, Monnat RJ, Jr. The Werner syndrome protein has separable recombination and viability functions. DNA Repair 2004;3:475–82.
18. Opresko PL, Calvo JP, von Kobbe C. Role for the Werner syndrome protein in the promotion of tumor cell growth. Mech Ageing Dev 2007;128:423–36.
19. Venkatesan RN, Treuting PM, Fuller ED, et al. Mutation at the polymerase active site of mouse DNA polymerase g increases genomic instability and accelerates tumorigenesis. Mol Cell Biol 2007;27:7669–82.
20. Kronmal RA. Spurious correlation and the fallacy of the ratio standard. J R Stat Soc Ser A 1993;156:379–92.
21. Jackson SP, Bartek J. The DNA-damage response in human biology and disease. Nature 2009;461:1071–8.
22. Nakamura AJ, Rao VA, Pommier Y, Bonner WM. The complexity of phosphorylated H2AX foci formation and DNA repair assembly at DNA double-strand breaks. Cell Cycle 2010;9:389–97.
23. Gebhart E, Bauer R, Raub U, Schinzel M, Ruprecht KW, Jonas JB. Spontaneous and induced chromosomal instability in Werner syndrome. Hum Genet 1988;80:135–9.
24. Ogburn CE, Oshima J, Poot M, et al. An apoptosis-inducing genotoxin differentiates heterozygotic carriers for Werner helicase mutations from wild-type and homozygous mutants. Hum Genet 1997;101:121–5.
25. Okada M, Goto M, Furuichi Y, Sugimoto M. Differential effects of cytotoxic drugs on mortal and immortalized B-lymphoblastoid cell lines from normal and Werner's syndrome patients. Biol Pharm Bull 1998;21:235–9.
26. Poot M, Gollahon KA, Rabinovitch PS. Werner syndrome lymphoblastoid cells are sensitive to camptothecin-induced apoptosis in S-phase. Hum Genet 1999;104:10–4.
27. Poot M, Yom JS, Whang SH, Kato JT, Gollahon KA, Rabinovitch PS. Werner syndrome cells are sensitive to DNA cross-linking drugs. FASEB J 2001;15:1224–6.
28. Poot M, Silber JR, Rabinovitch PS. A novel flow cytometric technique for drug cytotoxicity gives results comparable to colony-forming assays. Cytometry 2002;48:1–5.
29. Poot M, Gollahon KA, Emond MJ, Silber JR, Rabinovitch PS. Werner syndrome diploid fibroblasts are sensitive to 4-nitroquinoline-*N*-oxide and 8-methoxypsoralen: implications for the disease phenotype. FASEB J 2002;16:757–8.
30. Rodriguez-Lopez AM, Jackson DA, Iborra F, Cox LS. Asymmetry of DNA replication fork progression in Werner's syndrome. Aging Cell 2002;1:30–9.
31. Karmakar P, Bohr VA. Cellular dynamics and modulation of WRN protein is DNA damage specific. Mech Ageing Dev 2005;126:1146–58.
32. Davies SL, North PS, Dart A, Lakin ND, Hickson ID. Phosphorylation of the Bloom's syndrome helicase and its role in recovery from S-phase arrest. Mol Cell Biol 2004;24:1279–91.
33. Poot M, Hoehn H. DNA topoisomerases and the DNA lesion in human genetic instability syndromes. Toxicol Let 1993;67:297–308.
34. Rao VA, Fan AM, Meng L, et al. Phosphorylation of BLM, dissociation from topoisomerase IIIα, and colocalization with γ-H2AX after topoisomerase I-induced replication damage. Mol Cell Biol 2005;25:8925–37.
35. Marple T, Kim TM, Hasty P. Embryonic stem cells deficient for Brca2 or Blm exhibit divergent genotoxic profiles that support opposing activities during homologous recombination. Mutat Res 2006;602:110–20.
36. Parker WB, Cheng YC. Metabolism and mechanism of action of 5-fluorouracil. Pharmacol Ther 1990;48:381–95.
37. Wyatt M, Wilson D. Participation of DNA repair in the response to 5-fluorouracil. Cell Mol Life Sci 2009;66:788–99.
38. Davies SL, North PS, Hickson ID. Role for BLM in replication-fork restart and suppression of origin firing after replicative stress. Nat Struct Mol Biol 2007;14:677–9.
39. Du X, Shen J, Kugan N, et al. Telomere shortening exposes functions for the mouse Werner and Bloom syndrome genes. Mol Cell Biol 2004;24:8437–46.
40. Chang S, Multani AS, Cabrera NG, et al. Essential role of limiting telomeres in the pathogenesis of Werner syndrome. Nat Genet 2004;36:877–82.
41. Multani AS, Chang S. WRN at telomeres: implications for aging and cancer. J Cell Sci 2007;120:713–21.
42. Opresko PL. Telomere ResQue and preservation—roles for the Werner syndrome protein and other RecQ helicases. Mech Ageing Dev 2008;129:79–90.
43. Imamura O, Fujita K, Itoh C, Takeda S, Furuichi Y, Matsumoto T. Werner and Bloom helicases are involved in DNA repair in a complementary fashion. Oncogene 2002;21:954–63.
44. Kawabe Y, Seki M, Yoshimura A, et al. Analyses of the interaction of WRNIP1 with Werner syndrome protein (WRN) *in vitro* and in the cell. DNA Repair 2006;5:816–28.
45. Otsuki M, Seki M, Kawabe Y, et al. WRN counteracts the NHEJ pathway upon camptothecin exposure. Biochem Biophys Res Commun 2007;355:477–82.
46. Imamura O, Fujita K, Shimamoto A, et al. Bloom helicase is involved in DNA surveillance in early S phase in vertebrate cells. Oncogene 2001;20:1143–51.
47. Hayashi T, Seki M, Inoue E, et al. Vertebrate WRNIP1 and BLM are required for efficient maintenance of genome stability. Genes Genet Syst 2008;83:95–100.
48. Kudlow BA, Kennedy BK, Monnat RJ. Werner and Hutchinson-Gilford progeria syndromes: mechanistic basis of human progeroid diseases. Nat Rev Mol Cell Biol 2007;8:394–404.
49. Helleday T, Petermann E, Lundin C, Hodgson B, Sharma RA. DNA repair pathways as targets for cancer therapy. Nat Rev Cancer 2008;8:193–204.
50. Luo J, Solimini NL, Elledge SJ. Principles of cancer therapy: oncogene and non-oncogene addiction. Cell 2009;136:823–37.